9-15-2001

Bacterial RNase P holoenzyme crosslinking analysis reveals protein interaction sites on the RNA subunit

S. M. Sharkady

J. M. Nolan

Nucleic Acids Research

Article Navigation

Bacterial ribonuclease P holoenzyme crosslinking analysis reveals protein interaction sites on the RNA subunit

Stephen M. Sharkady, James M. Nolan

Nucleic Acids Research, Volume 29, Issue 18, 15 September 2001, Pages 3848–3856,
https://doi.org/10.1093/nar/29.18.3848

Published: 15 September 2001

Abstract

The structure of the *Escherichia coli* ribonuclease P (RNase P) holoenzyme was investigated by site-directed attachment of an aryl azide crosslink reagent to specific sites in the protein subunit of the enzyme. The sites of crosslinking to the RNase P RNA subunit were mapped by primer extension to several conserved residues and structural features throughout the RNA. The results suggest rearrangement of current tertiary models of the RNA subunit, particularly in regions poorly constrained by earlier data. Crosslinks to the substrate precursor-tRNA were also detected, consistent with previous crosslinking results in the *Bacillus subtilis* RNase P holoenzyme.

Received June 14, 2001; Revised and Accepted July 24, 2001.

INTRODUCTION

Ribonuclease P (RNase P) is an essential bacterial enzyme which functions to produce mature transfer RNAs (mat-tRNAs) by cleaving 5′ sequences of precursor tRNAs (pre-tRNAs). The RNase P holoenzyme from *Escherichia coli* consists of a large RNA subunit of 377 nt (140 kDa) and a small protein subunit of 119 amino acids (14 kDa). The RNA is the catalytic component of the holoenzyme and can produce mature tRNAs *in vitro* under high salt conditions, in the absence of protein. However, the protein subunit is required for catalytic activity *in vitro* under physiological conditions (1,2) and is essential *in vivo* for viability (3,4). The protein subunit increases the catalytic efficiency of the reaction by specifically enhancing affinity for substrate (5) and by speeding up the rate-limiting step of product release (6). The protein subunit also increases the affinity of RNase P RNA for substrates other than pre-tRNA, such as 4.5S RNA (2).

In recent years, structural data on the RNase P protein subunit has become available. The crystal structure of the protein from *Bacillus subtilis* (7) revealed a mixed α–β protein with an unusual left-handed β–α–β turn, similar to two other RNA binding protein's domains, domain II of ribosomal protein S5 and domain IV of elongation factor EF-G. A three-dimensional NMR structure of the RNase P protein from *Staphylococcus aureus* revealed architecture similar to the RNase P protein from *B.subtilis* (8). The RNase P RNA subunit has eluded crystallization, but has proven amenable to crosslinking; three-dimensional models of the RNA subunit from both *E.coli* and *B.subtilis* were created based on the phylogenetically derived secondary structure. Intramolecular and intermolecular crosslinking between the RNA subunit and the pre-tRNA substrate provided distance constraints for modeling (9–11).

Even with the structure of the protein subunit known and a working model of the RNA subunit constructed, the specific binding surface between subunits remains ill defined. Hydroxyl radical and nuclease footprinting experiments using the holoenzyme from *B.subtilis* showed three regions of the P RNA sequence protected in the presence of the protein subunit (12). Footprinting studies have also been conducted on the *E.coli* holoenzyme using enzymatic probes (13,14). More recently, the protein-binding site on the RNA has been probed by tethering a Fe–EDTA cleavage compound to the protein subunit (15). However, there is no clear consensus among these studies. The nature of the interaction between the RNase P protein and the substrate pre-tRNA has been investigated by crosslinking as well. Site-directed crosslinks from the *B.subtilis* protein subunit to pre-tRNAs with varying 5′ leader lengths showed that the precursor sequence lies across the central cleft of the RNase P protein β-sheet (16) (Fig. 1).

The purpose of the present study was to determine the protein interaction sites on the RNA subunit. To address this question, a thiol-specific, photoactive crosslinking reagent, azidophenacyl bromide (APB), was conjugated to a cysteine residue introduced at specific sites within the RNase P protein. The modified protein could then be incubated with RNase P RNA and crosslinked by UV irradiation. The sites of crosslinking on the RNA were mapped by primer extension to reveal regions of the RNA that interact with the protein.

MATERIALS AND METHODS

Mutagenesis

Site-directed mutagenesis was performed according to the QuickChange protocol, using *Pfu* DNA polymerase (Stratagene). The native cysteine was mutated to alanine (C113A). The C113A mutant was then used to construct second-site mutations F18C/C113A, H78C/C113A or R99C/C113A.

Primers

F18Cfor: 5′-CTCCCAGTCAATGCACATTCGTTTTCCAGCAGC-3′; F18Crev: 5′-GCTGCTGGAAAACGAATGTGCATTGACTGGGAG-3′; H78Cfor: 5′-CGTCTGCGCCAATGTGAACTCCCGG-3′; H78Crev: 5′-CCGGGAGTTCACATTGGCGCAGACG-3′; R99Cfor: 5′-GACCTCGATAACTGTGCTCTCTCGGAA-3′; R99Crev: 5′-CTTCCGAGAGTGCACAGTTATCGAGGTC-3′; C113A/BglIfor: 5′-CGCCGCCACGCCCGCCTGGCTCGCG-3′; C113A/BglIrev: 5′-CGCGAGCCAGGCGGGCGTGGCGGCG-3′; KS: 5′-TCGAGGTCGACGGTATC-3′; Ec225rev: 5′-GGGTGGAGTTTACCGTGC-3′.

Preparation of RNA

All RNAs were transcribed from linearized plasmid templates using T7 RNA polymerase. The template for RNase P RNA transcription for analytical crosslink studies was plasmid p98SX linearized with *Xho*I. p98SX was constructed from pDW27 (17) by digestion with *Sna*BI and *Xho*I, filled in with Klenow fragment of DNA polymerase I and dNTPs and religated to produce p98SX. To make P RNA for primer extensions, RNase P was transcribed from *Xho*I-digested pecKS, which yields RNA with a 26 nt 3′ extension complementary to the pBluescript KS primer (18). Substrate pre-tRNA ^{Asp}

from *B.subtilis* containing a 33 nt 5′ leader sequence was transcribed from plasmid pDW152 (17) digested with *Bst*NI. *Bacillus subtilis* pre-tRNA^{Asp} containing a 2, 3 and 4 base 5′ leader was transcribed from plasmids ptR2D, ptR3D and ptR4D, respectively, each digested with *Bst*NI (16) (plasmids ptR2D, ptR3D and ptR4D were graciously provided by Dr Carol Fierke, University of Michigan). All transcriptions contained 2.5 U/μl of T7 RNA polymerase, 2 mM each GTP, ATP, UTP and CTP, except reactions with [α-^{32}P]GTP (Amersham) for which [GTP] was 0.5 mM. RNA transcripts were gel purified (P RNA on a 4% acrylamide/8 M urea/TBE gel, pre-tRNA on an 8% acrylamide/8 M urea/TBE gel), detected by UV shadow, excised, eluted passively with 0.5 M ammonium acetate, 0.1% sodium dodecyl sulfate (SDS) in 1× TE and ethanol precipitated. RNA concentrations were calculated by using either the absorbance at 260 nm (32 μg/OD), or by specific activity for labeled RNA samples.

Protein purification

RNase P protein from *E.coli* was expressed from plasmid pQE30EcoPprotein (19) as an N-terminal 6-his fusion. A culture of DH5α (20) cells containing pQE30EcoPprotein was grown to an OD_{600} of 0.7 and then induced with 0.5 mM isopropyl-β-D-thiogalactopyranoside for 3 h at room temperature. Cells were centrifuged at 3800 *g* for 15 min at 4°C. Protein was purified under denaturing conditions using Ni^{2+}-NTA spin columns (Qiagen) according to the manufacturer's directions using 6 M GuHCl, 10 mM Tris–HCl and 10 mM $NaH(PO_4)$ pH 8.0 (Buffer A) for lysis. Columns were washed with Buffer C [8 M urea, 10 mM Tris–HCl and 10 mM $NaH(PO_4)$, pH 6.3]. P protein was eluted in two fractions of 0.2 ml each of Buffer E [8 M urea, 10 mM Tris–HCl and 10 mM $NaH(PO_4)$, pH 4.5], analyzed by Tris–tricine SDS–polyacrylamide gel electrophoresis (PAGE) (21) and pooled. RNase P protein was renatured by serial dialysis using micro dialysis cassettes (Pierce) from protein buffer [50 mM *N*-[hydroxyethyl]piperazine-*N*′-[2-ethanesulfonic acid] (HEPES) pH 8.0, 50 mM NaCl, 0.05% IGEPAL] containing 4 M urea, followed by protein buffer plus 2 M urea and two changes in protein buffer without urea plus 20% glycerol. Protein was quantitated by the Coomassie dye-binding method (22), using bovine serum albumin as a standard.

Protein modification

Proteins were modified with the heterobifunctional crosslinking reagent APB (Fluka). Modification reactions contained 100 μM protein, 3 mM APB, in protein buffer plus 20% glycerol and 0.5 mM Tris[2-carboxyethylphosphine] HCl, a non-thiol reducing reagent (Pierce). An equal volume of 8 M urea was added and the reaction was incubated on ice in the dark for 4 h. The excess APB was quenched by the addition of 4 mM β-mercaptoethanol and incubated on ice for 30 min. Modified proteins were then renatured and unconjugated APB removed by dialysis as described above.

Activity assays

RNase P RNA was annealed by heating to 80°C for 2 min in 25 mM HEPES pH 8.0, 50 mM NH_4Cl, 0.025% IGEPAL, room temperature for 2 min, followed by 50°C for 10 min (23). RNase P RNA was diluted into 1× reaction buffer (50 mM HEPES pH 8.0, 100 mM NH_4Cl, 10 mM $MgCl_2$, 0.05% IGEPAL) then mixed with RNase P protein in reaction buffer and incubated at 37°C for 5 min. Substrate pre-tRNA was incubated separately in reaction buffer at 37°C for 5 min, then

added to enzyme to start reactions. Final reactants were 0.5 nM RNA, 1 nM protein, 20 nM pre-tRNA. Reactions (10 µl) were stopped after 15 min at 37°C by addition of an equal volume of 1× TBE, 50 mM EDTA, 8 M urea, 0.01% bromophenol blue, 0.01% xylene cyanol; reactions were then heated to 80°C, quick chilled on ice, then resolved on 8% polyacrylamide/8 M urea/TBE gels and quantitated using a Fuji phosphorimager.

Preparative and analytical protein crosslinking to RNase P RNA

RNase P RNA was annealed by heating to 80°C for 2 min, room temperature for 2 min, 50°C for 10 min and then placed on ice until use (23). RNase P RNA and modified protein were incubated in 400 mM NH_4Cl, 50 mM HEPES pH 8.0, 10 mM $MgCl_2$ and 0.05% IGEPAL (v/v) at 37°C for 5 min, then irradiated in open Eppendorf tubes for 15 min at room temperature with a 302 nm hand held lamp (UVP) at 4 cm using a polystyrene filter. For analytical crosslinks 20 nM RNA was reacted with 40 or 80 nM protein in 10 µl. Protease K treatments were performed by addition of 1 µl of 20 µg/ml protease K and incubation at 37°C for 20 min. Reactions were stopped by the addition of an equal volume of stop solution (1× TBE, 8 M urea, 50 mM EDTA, 0.01% bromophenol blue, 0.01% xylene cyanol and 0.2% SDS). For preparative reactions, 400 nM P RNA was incubated with 400 or 800 nM modified protein and reacted in 200 µl; preparative reactions were made 0.2% in SDS, precipitated with EtOH, resuspended in 10 µl TE followed by addition of 10 µl of stop solution. The crosslinks were resolved on a 4% acrylamide/8 M urea/TBE gel. Analytical crosslink gels were fixed, dried and quantitated by phosphorimager (Fuji). Preparative gels were visualized by staining with Sypro Green RNA stain (Molecular Probes); crosslinked and uncrosslinked RNAs were passively eluted and precipitated as above.

Primer extension analysis

Gel purified protein–RNA crosslinked species were analyzed by primer extension using primers that cover the entire P RNA sequence. Primers were 5′ end-labeled with [γ-^{32}P]ATP (Amersham) using T4 polynucleotide kinase (Gibco BRL). End-labeled primer (5 pmol) was annealed to RNA samples (0.2 pmol) in 50 mM Tris–HCl (pH 8.3 at 42°C) and 25 mM KCl at 90°C for 2 min then slowly cooled to 30°C. Extension reactions were carried out in 50 mM Tris–HCl (pH 8.3 at 42°C), 50 mM KCl, 10 mM dithiothreitol, 10 mM $MgCl_2$ and 200 µM of each dNTP plus 1 U avian myeloblastosis virus reverse transcriptase (Seikagaku)/7.5 µl reaction at 42°C for 1 h. Reactions were terminated by the addition of 0.8 vol of stop solution containing 85% formamide, 20 mM EDTA, 0.1% bromophenol blue and 0.1% xylene cyanol. The labeled extension products were resolved on 6% acrylamide/8 M urea/TBE gels, fixed, dried and visualized by autoradiography. Sequencing reactions were as described above, using non-irradiated RNA and a final concentration of 10 µM of the appropriate ddNTP.

Crosslinking of P protein mutants to pre-tRNAs with varying 5′ leader lengths

Reactions were similar to protein–P RNA crosslinks, but buffer pH was 6.0 and calcium was substituted for magnesium to minimize cleavage of pre-tRNA (24,25). RNase P RNA was annealed prior to use as described above. Samples (400 nM) of RNase P RNA and (400 nM) APB-modified F18C/C113A or H78C/C113A P protein mutant were incubated at 37°C for 10 min in 400 mM NH_4Cl, 50 mM HEPES pH 6.0, 10 mM $CaCl_2$ and 0.05% IGEPAL (v/v). Pre-tRNA was pre-

incubated separately in the same buffer at 37°C for 10 min then mixed with holoenzyme and incubated for an additional 10 min at 37°C. The reactions were irradiated with 302 nm UV light using a polystyrene filter for 15 min at room temperature. Protease K treatments were performed as above. An equal volume of SDS sample buffer (100 mM Tris pH 6.8, 0.02% SDS, 0.2 M β-mercaptoethanol, 20% glycerol and 50 mM EDTA) was added; the samples were then resolved on a 15% acrylamide Tris–glycine SDS–PAGE gel (26), fixed, dried and visualized on a Fuji phosphorimager.

Homology modeling

The crystal structure coordinates of the RNase P protein from *B.subtilis* were obtained from the RCSB [http://www.rcsb.org/pdb /, accession no. 1A6F (7)] and used as a template for modeling the *E.coli* RNase P protein using SwissPdbViewer version 3.5 (http://www.expasy.ch/spdbv/mainpage.ht m).

RESULTS

Confirmation of P protein mutants and modifications

Residues on the P protein to be replaced with cysteine and modified with crosslinker were chosen using a homology model of the *E.coli* P protein based on the crystal structure of the *B.subtilis* P protein (7). Amino acids H78 and R99 were also chosen due to their close proximity to highly conserved regions in the bacterial P proteins, their high probability of being surface exposed based on the homology model, and their distribution over the surface of the P protein. Amino acid F18 was chosen based on the observation that the homologous residue in the *B.subtilis* P protein, F16, crosslinks to precursor sequences ≥4 nt in pre-tRNA (16), thus it was expected to form the homologous crosslink in the *E.coli* holoenzyme. The thiol-specific aryl azide crosslinking reagent, APB, was utilized for attachment of photoagent at the desired sites. The natural protein sequence has a single cysteine, C113. For introduction of a unique thiol at F18, H78 or R99, the natural cysteine was mutated to alanine by site-directed mutagenesis (C113A), then individual second-site mutations, F18C/C113A, H78C/C113A and R99C/C113A, were generated in the C113A background. The activity of protein mutants was assessed to determine if the newly introduced cysteine or subsequent modification with APB perturbed the native structure of the P protein. Mutant proteins were tested for their ability to promote cleavage of substrate in the holoenzyme under multiple turnover conditions in buffer containing 100 mM NH_4Cl, 10 mM $MgCl_2$ and 20 nM pre-tRNA substrate, in which P RNA alone is enzymatically inactive. All mutants, both unmodified and modified with APB, promoted cleavage of pre-tRNA by RNase P RNA at near wild-type levels (Table 1).

Crosslinking of mutant P proteins to pre-tRNAs with varying 5′ leader lengths

A previous study demonstrated that residue F16 of *B.subtilis*, when changed to cysteine and modified with APB, crosslinks to pre-tRNA substrates with ≥4 nt leader sequences (16). The homologous residue in the *E.coli* P protein, F1 was tested for the ability to crosslink to pre-tRNAs with 5′ leaders of 2, 3 or 4 bases in length. In addition to F18, H78 was also used as a negative control, as it is located on the opposite face of the P protein from F18 and the proposed substrate-binding site. Figure 2 shows the crosslinking results for the mutant holoenzymes F18C/C113A and H78C/C113A,

modified with APB, to pre-tRNAs. Reactions contained 400 nM each P RNA and modified protein, except for control reactions. A small amount of non-specific crosslinking of protein to pre-tRNA in the absence of P RNA was seen as a faint smear (Fig. 2, lanes 2 and 3). Specific crosslinks were detected between F18C/C113A and both 3 and 4 nt leader pre-tRNA (Fig. 2, lanes 11 and 15, respectively, compare with lane 6, pre-tRNA with leader of 2 bases). The bands are protein–RNA crosslinks as evidenced by sensitivity to protease K treatment (Fig. 2, compare lanes 11 and 12, 15 and 16). F18C/C113A crosslinked to a pre-tRNA with either 3 or 4 base leader with an efficiency of 0.5%, crosslinking to the 2 base leader tRNA was only 0.1%. The specificity of the reaction agrees well with previous results, although the efficiency of crosslinking differs greatly. The *B.subtilis* F16C protein crosslinked to pre-tRNA at 15% efficiency (16). H78C/C113A did not crosslink to any of the pre-tRNAs tested (Fig. 2, lanes 9, 13 and 17). This agrees with the *B.subtilis* system, as H78 lies outside the proposed substrate-binding cleft.

Analytical crosslinking to RNase P RNA

The ability of the P protein variants to crosslink to P RNA and their relative crosslinking efficiencies were tested. Crosslink reactions were carried out in 400 mM NH_4Cl reaction buffer, the optimal monovalent salt concentration for protein-binding specificity to P RNA (27). RNA (20 nM) was incubated with 40 or 80 nM modified protein and irradiated at 302 nm for 15 min. Protein–P RNA crosslinks run as a smear just below the well in the 4% acrylamide/8 M urea/TBE gel system (Fig. 3). The protein–RNA crosslink bands were confirmed by sensitivity to protease K treatment (compare lanes 3 and 4 for F18C/C113A, lanes 7 and 8 for H78C/C113A, lanes 11 and 12 for R99C/C113A), and UV dependence (Fig. 3, compare lanes 2 and 3, 6 and 7, or 10 and 11). Crosslinking efficiency was dependent upon protein concentration. When reactions were performed using 20 nM each of protein and RNA, crosslinking efficiencies were 2.9% for F18C/C113A, and 1.0% each for H78C/C113A and R99C/C113A (Table 1). The native RNase P protein, C113, was also modified and crosslinked, but the efficiency was <0.1%, even using 4-fold excess protein (Table 1 and data not shown).

Primer extension analysis of P protein to native P RNA crosslinks

Preparative crosslinking reactions contained 400 nM P RNA and 400 or 800 nM protein. Reconstituted holoenzyme was irradiated with 302 nm UV light to activate the aryl azide, causing a crosslink to nucleotides of the RNA subunit that are in close proximity. Protein–P RNA crosslinked species were then isolated by gel purification, eluted and subjected to primer extension analysis. The two primers used for primer extensions were KS, which is complementary to the extended 3′ end of pecKS P RNA, and Ec225r, which is complementary to bases 242–225 of P RNA. The primers chosen allowed analysis of the entire sequence of P RNA. Reverse transcriptase extends the labeled primer up to the nucleotide 3′ to the crosslink site (28). Examples of crosslinks seen for the three mutants are illustrated in Figure 4A and B. Crosslinks can be se stops in the primer extensions not seen in the control lanes (C). Primer extension stop sites were screened by several criteria: (i) the relative intensity of the crosslink stop compared with stops seen for control uncrosslinked RNA from the same crosslink reaction in the adjacent lane. This control distinguishes crosslinks from reverse transcriptase pause sites, which are presumed to be caused by secondary structure. (ii) Crosslinks were also evaluated for dependence on protein concentration. Sites of crosslinking detected at equimolar protein:RNA ratios are more likely to represent a high-affinity binding site compared to those that require excess protein for maximal detection. (iii) Crosslinks were also assessed for reproducibility; those sites noted were detected in at least three separate experiments. Consequently, the sites noted are a

conservatively chosen set of strong crosslink sites. Weaker crosslinks, such as those requiring excess protein for maximal detection, are also apparent. The weaker sites may also represent valid crosslinks, but we are most confident of the strongest sites. The position of the crosslinks in RNase P RNA was determined by the sequencing ladder in adjacent lanes. All three modified protein mutants crosslinked to bases C228 in helix P11 and U231 in J14/11. [In *E.coli* RNase P RNA, base-paired helices are numbered P1–P18 in 5′–3′ order. Unpaired 'joining' regions are denoted with J and the number of flanking helices in 5′–3′ order (29).] H78C also crosslinked to G246 and C247 at the junction of helix P5 and J5/15, to C131 in J11/12 and to U167–C168 in helix P12. The sites of crosslinking for each of the three protein mutants, F18C, H78C and R99C, are compiled in Table 1. The crosslink sites are also mapped onto the revised secondary structure of *E.coli* RNase P RNA (11,30) and the Type A RNase P RNA minimum consensus sequence (31) in Figure 5. The crosslink sites cluster in three regions of the secondary structure of *E.coli* RNase P RNA.

DISCUSSION

We determined regions of RNase P RNA that interact with the protein subunit utilizing site-specific protein–P RNA crosslinking. The results of our analytical crosslink studies of holoenzyme containing modified F18C/C113A protein to pre-tRNA substrate are in general agreement with similar studies performed with the homologous residue of *B.subtilis* P protein, F16C. The *B.subtilis* F16C crosslinked to substrate tRNAs with 5′ precursor sequences ≥4 nt, but not to 2 or 3 nt precursors. Crosslinkers outside the central binding cleft determined in *B.subtilis* did not crosslink to pre-tRNA. We saw similar results for *E.coli* F18C/C113A, although crosslinking was detected to both 3 and 4 nt precursors. In addition, *E.coli* H78C/C113A, which is predicted to be located outside the corresponding binding cleft in *E.coli*, did not crosslink to pre-tRNA as expected. The most striking difference between the two systems is a difference in crosslink efficiency. The differences in efficiency between the two systems are likely due to inherent differences in reactivity or solubility of the protein from the two species.

Given that the protein–tRNA crosslinks agreed well with those seen in *B.subtilis*, the relative efficiency of the protein–P RNA reactions compared with the specific reaction seen for F18C/C113A with pre-tRNA suggests that the protein–P RNA crosslinks also represent specific P RNA–protein interactions. Most of the crosslinks that we observed from the P protein mutants to P RNA were in or adjacent to highly conserved regions and near the active site of RNase P RNA. The crosslinks are mapped onto the secondary structure consensus of Type A RNase P RNAs (Fig. 5B). We observed that F18C, H78C and R99C crosslinked to bases C228 and U231, which are conserved positions in J14/11 and P11 of all bacterial P RNAs. H78C also crosslinked to positions C131, U167, C168, G246 and C247 of the P RNA. The G246 crosslink site observed for H78C in P5 is 100% conserved in all Type A bacterial RNase P RNAs (31) and is believed to be near the active site (32). C131 is >98% conserved in all Type A bacterial RNase P RNAs; nucleotide 231 is conserved as a pyrimidine in 98% of Type A RNAs. Nucleotides 167 and 168 are part of a highly variable region of P12 directly adjacent to the more conserved base of the highly conserved P12 helix.

The bacterial RNase P protein is predicted to lie near the active site of the RNA subunit, based upon the ability of the protein to crosslink to precursor sequences of the substrate near the cleavage site. In the model of pre-tRNA binding to P protein, conserved residues near H78 are closest to the site of cleavage of the pre-tRNA substrate (16). Our data are

consistent with this model and the large body of tRNA–P RNA crosslink data that identify residues at or near the active site of the ribozyme. Specifically, an aryl azide attached to the 5′ end of mat-tRNA, the site of action of RNase P, crosslinked to nucleotides 231 and 248 (32). Our crosslinks to nucleotides 228, 231, 246 and 247 are in close agreement with these sites. These regions have also been shown to interact with tRNA in nuclease (33) and chemical cleavage (34) protection assays.

The degree of overlap in our RNA crosslinks among the different protein mutants was somewhat surprising. However, distances between the different sites on the protein to which the aryl azide was attached are relatively small: the Cα of F18C is 23 Å from H78 and 27 Å from R99. H78C is 18 Å from R99. These distances are less than twice the distance between the Cα of cysteine and the reactive nitrene (14 Å), thus the crosslinker attached at any chosen residue could attack the same point in space. Our results illustrate the relatively small size of the P protein compared with RNase P RNA. The conserved regions of the protein likely to interact with RNase P RNA are clustered in a small region of this already small protein (β strand 3 and helix 2, see Fig. 1). The natural cysteine, C113 failed to crosslink to P RNA and lies on the opposite side of the protein with fewer conserved residues.

The RNA target for the crosslink is likely to have contributed to the clustering of crosslinks sites observed. All of the crosslinked nucleotides are unpaired or adjacent to unpaired residues in the secondary structure. None are in the middle of helices. A similar trend can be seen in the wealth of RNA–RNA crosslink data available using APB. Of the RNA–RNA crosslinks characterized, <10% are in helices, compared with the expected 35% (compiled from 9,10,18,32,35,36). Thus, APB may not efficiently crosslink to A-form helical regions in close proximity, but instead reacts with adjacent unpaired residues. The size of the nucleotide target may also lead to clustering of crosslinks. Nucleotides range in size from 10 to 14 Å so modified proteins crosslinking to the same nucleotide need not react with the same atom at a particular point in space. The protein–RNA crosslink sites detected do not appear to be intrinsically reactive nucleotides, as excess APB-cysteine in solution did not have enhanced reactivity to the RNA crosslink sites (data not shown).

One test of the validity of detected crosslinks is to demonstrate that the crosslinked species are active. This is a technical challenge, as current gel systems do not allow us to resolve different protein–RNA crosslinks from each other. However, we were able to detect active crosslinks using a self-cleaving P RNA–tRNA chimera, TPT118. This RNA consists of a pre-tRNA mini helix tethered to a circularly permuted P RNA at nucleotide 118 (37). TPT118 is able to self-cleave the 5′ precursor sequence, but activity is stimulated 30-fold in the presence of protein (J.M.Nolan, unpublished data). Modified protein was incubated with TPT118 in the presence of calcium to allow interaction of subunits with minimal cleavage of the RNAs, the protein was crosslinked to RNA with UV light, and uncrosslinked protein was removed by extensive washing with buffer lacking calcium. Addition of magnesium allowed RNA self-cleavage. The self-cleaved, crosslinked RNAs were purified by gel electrophoresis and mapped by primer extension. Crosslinks to residues 246 and 247 by F18C and H78C were confirmed in this manner (data not shown).

Our results are in partial agreement with previous observations of regions of the P RNA, which interact with the protein. Chemical cleavage footprinting (12) of the *B.subtilis* holoenzyme showed that the P protein protected three main regions on the RNA subunit. The corresponding regions in *E.coli* P RNA are shown shaded in Figure 5B. The previous results and ours indicate P12 as part of the protein-binding site, although we were not able to confirm other regions protected in the

previous study, such as P2 and P8–P9. More recently, the site of *E.coli* P RNA that interacts with the protein subunit was investigated by tethering an Fe–EDTA cleavage compound to specific sites on the P protein. Again, our results are in partial agreement with this study. Crosslinks we detected for H78C to nucleotides 246 and 247 are directly adjacent in the secondary structure to sites in helix P4, which were cleaved by Fe–EDTA attached to residue 54. Residue K54 is predicted to lie between H78 and F18 in the three-dimensional structure of the P protein. However, none of our other crosslink sites coincide with Fe–EDTA cleavage sites from the previous study.

The *B.subtilis* RNase P holoenzyme has recently been shown to form a $(protein)_2(RNA)_2$ tetramer *in vitro*, while the RNA subunit alone exists as a monomer (38). The *E.coli* RNA did not form a heterotetramer with the *B.subtilis* protei but instead formed a higher order aggregate. The *E.coli* RNA was able to compete efficiently with the *B.subtilis* RNA for binding to the *B.subtilis* protein, inhibiting formation of the *B.subtilis* tetramer (38). It is possible that the *E.coli* RNas RNA can form a similar tetramer in the presence of the *E.coli* protein. Alternatively, the difference in the behavior of the *E.coli* versus *B.subtilis* RNAs could result from differences in the secondary structure of the RNAs, which in turn could affect their ability to form a stable, symmetrical tetramer. It is thus unclear how our results should be interpreted with respect to the *B.subtilis* tetramer.

There are presently two different models of the *E.coli* RNase P RNA structure (9,11). Many of the crosslink sites detect in the present study were not modeled by Chen *et al.* (9), due to lack of sufficient structural constraints. In the Massire model (11), our crosslink sites cluster in two to three areas (Fig. 6). This may be due to uncertain placement of poorly constrained regions such as P12, or may in fact reflect two distinct binding sites necessary for tetramer formation. Our results suggest that several regions of the RNA subunit, previously not well defined by crosslinking to a specific region, need to be reoriented. The arrow in Figure 6 shows the proposed reorientation of helix P12. While the loop of P12 is likely peripheral, given its variable length, the base of this helix is well conserved and should be placed nearer the core of the enzyme. Similarly, P11 appears to interact with both protein and substrate and should be positioned near the core. The RNA–protein crosslink sites detected here will provide additional constraints for further modeling of the structure of RNase P RNA and help to determine the protein-binding site on the RNA.

ACKNOWLEDGEMENTS

We thank Drs Carol Fierke, David Engelke, Norm Pace, Sam Landry and Bill Wimley for helpful comments. We thank Drs Carol Fierke, Norm Pace, Barbara Vold and Rafael Rivera-Leon for supplying essential reagents. We also thank Sumit Borah and Chris Darcey for reading the manuscript. This material is based upon work supported by the National Science Foundation under Grant No. MCB-9631039 and by the Tulane Cancer Center.

* To whom correspondence should be addressed. Tel: +1 504 584 2453; Fax: +1 504 584 2739; Email: jnolan@tulane.edu

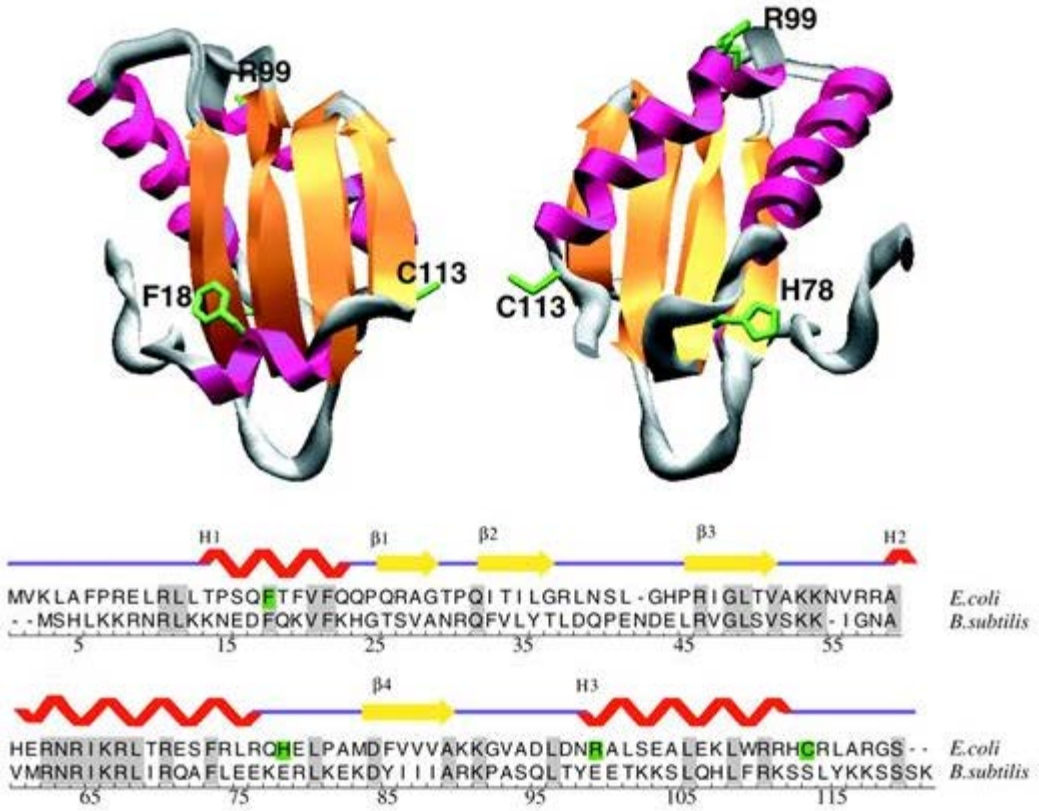

Open in new tab Download slide

Figure 1. A homology model of *E.coli* RNase P protein created using SwissPdbViewer and the crystal structure of the RNase P protein from *B.subtilis*. β strands are colored yellow, α helices are red. Two views are shown rotated 180° about the *y*-axis. The residues changed to cysteine in this study and the native cysteine, C113, are shown in green wireframe and labeled. Below is a sequence alignment of the *E.coli* and *B.subtilis* P protein sequences generated using SeqApp (D. Gilbert, Indiana University) from the WIT alignment of bacterial RNase P proteins (http://wit.integratedgenomics.com/IGwit/). The sites of mutation are highlighted in green, identical residues between proteins are highlighted in gray. The alignment is numbered below according to the *E.coli* sequence. The secondary structure elements that correspond to the sequence are indicated above the sequence with the same color coding for secondary elements as the tertiary model.

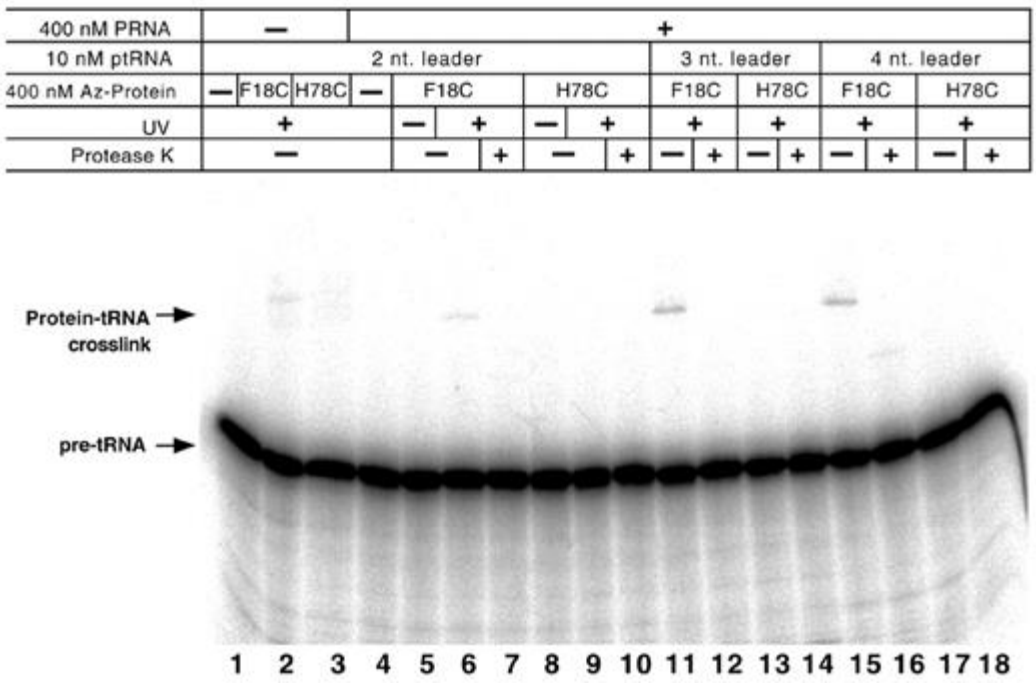

Open in new tab Download slide

Figure 2. Crosslinking analysis of P protein mutants F18C/C113A and H78C/C113A to pre-tRNAs with varying 5′ leader lengths. Modified P protein and P RNA (400 nM each) were incubated prior to the addition of pre-tRNA (10 nM). Samples were separated on a Tris–glycine 15% SDS–PAGE gel. Protein–RNA crosslinks and uncrosslinked RNA are labeled. The length of the pre-tRNAs 5′ leader used is denoted as –2, –3 or –4 from the site of cleavage.

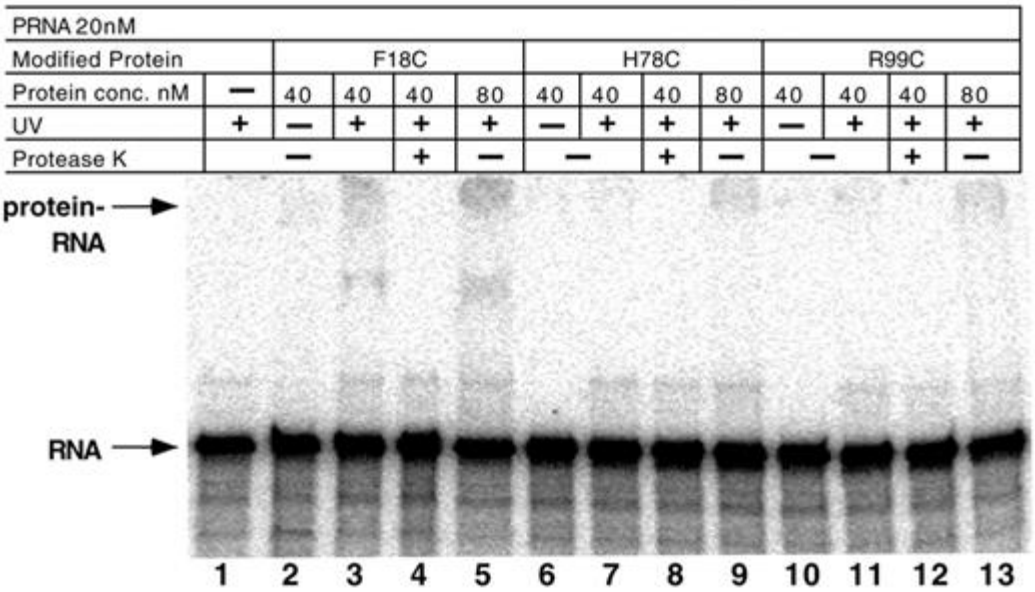

Open in new tab Download slide

Figure 3. Analytical crosslinking gel of modified P protein mutants to RNase P RNA. RNA and protein were

pre-incubated at 37°C for 10 min in 400 mM NH_4Cl, 50 mM HEPES pH 8.0, 10 mM $MgCl_2$ and 0.05% IGEPAL (v/v) followed by a 15 min irradiation with 302 nm UV light and separated on a 4% acrylamide/8 M urea/TBE gel. Protein–RNA crosslinks and uncrosslinked RNA bands are labeled.

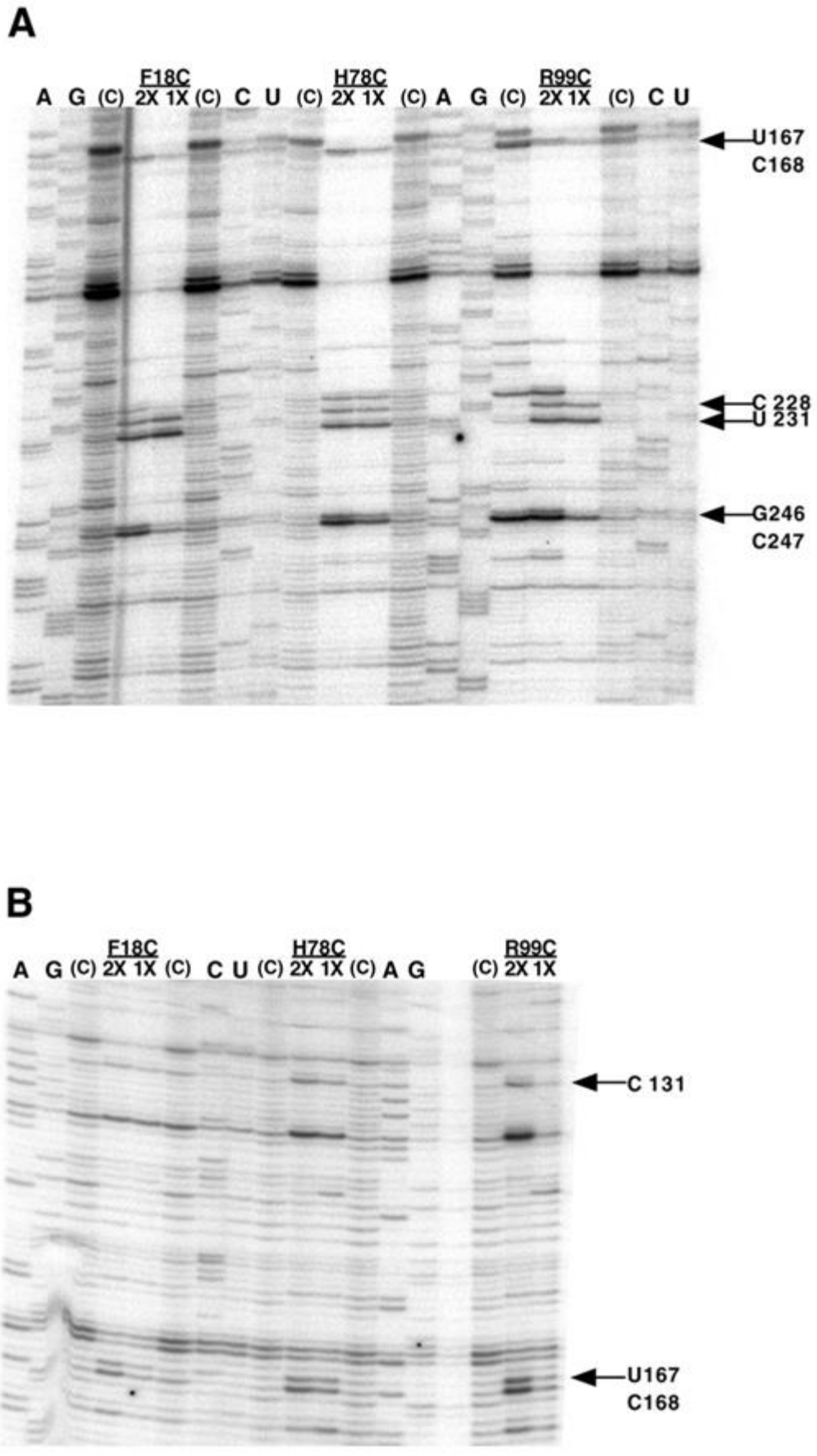

Open in new tab Download slide

Figure 4. Primer extension analysis of mutant P protein crosslink sites on *E.coli* RNase P RNA. Gel purified,

crosslinked species were extended with reverse transcriptase using the KS primer (**A**) and primer Ec225r (**B**). Extension products were analyzed on 6% acrylamide/8 M urea/TBE gels and visualized by autoradiography. Control lanes contain uncrosslinked, irradiated RNA as template and are labeled '(C)'. Ratios of protein:RNA of 1:1 and 2:1 were used in the crosslinking reactions and denoted as 1X and 2X, respectively, along with the P protein mutant used. The sequencing ladder reactions were generated by addition of ddNTPs to reverse transcriptase reactions and are labeled with the corresponding template nucleotide in the RNA. Sites of crosslinking are labeled as deduced from the sequencing reactions.

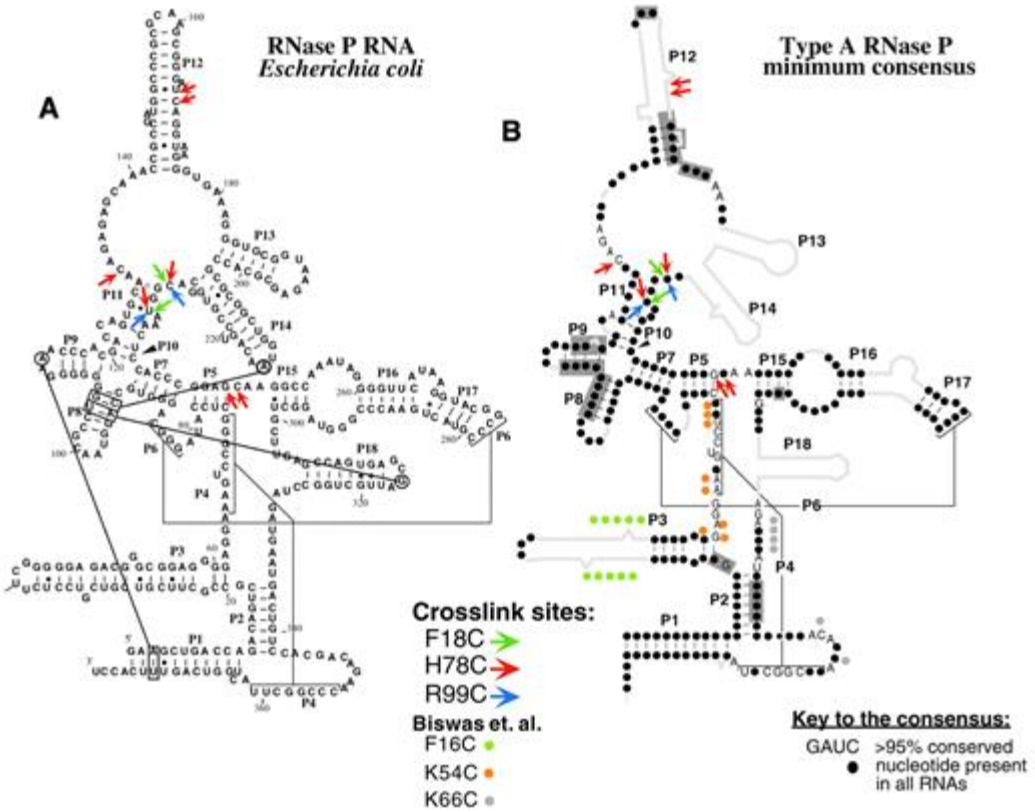

Open in new tab Download slide

Figure 5. Sites of crosslinking mapped onto (**A**) the refined secondary structure of *E.coli* RNase P RNA (30), (**B**) the minimum consensus for Type A bacterial RNase P RNAs. Sites of crosslinking are denoted by arrows and color coded: green, F18C; red, H78C; blue, R99C. (B) Shaded regions are the sites in *E.coli* P RNA homologous to sites of *B.subtilis* P RNA protected from hydroxyl radical and nuclease cleavage by *B.subtilis* P protein (12). The results of Fe–EDTA protein tether experiments (15) are shown as color circles: green, S16C; orange, K54C; gray, K66C.

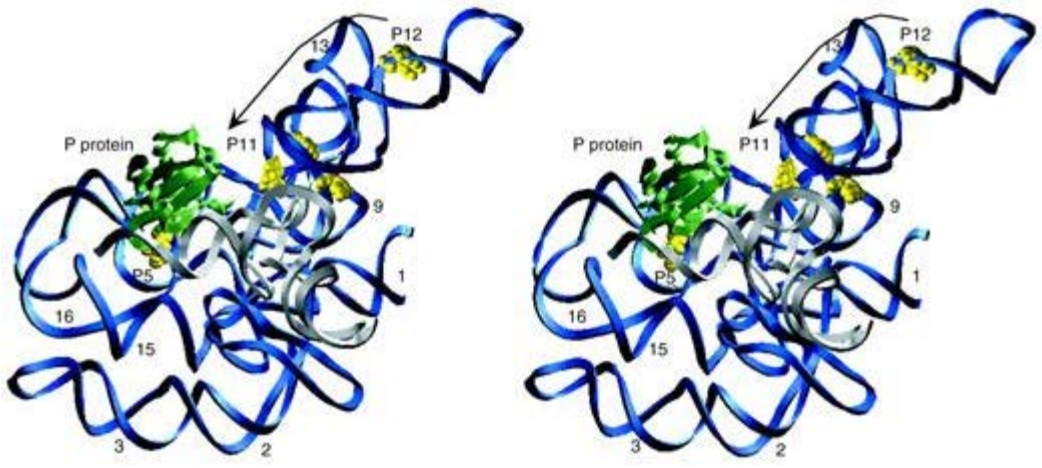

Open in new tab Download slide

Figure 6. Stereo view of sites of crosslinking for F18C, H78C and R99C mapped onto a model of *E.coli* RNase P RNA (11). The backbone of the RNase P RNA is shown in blue, bases involved in crosslinks with F18C, H78C and R99C P proteins are displayed in yellow spacefill. tRNA substrate is shown in gray. The RNase P protein is shown for scale in green. The arrow indicates direction of proposed reorientation of helix P12. Helices which crosslink to protein are denoted P5, P11 and P12. Other helices are also noted by numerals only.

Table 1.

RNase P protein activity and crosslink data

Protein	Percent wt activity (%)		Percent RNase P RNA crosslinked (%)	RNase P RNA site crosslinked
	Unmodified	Azido		
F18C/C113A	30	60	2.9	C228, U231
H78C/C113A	90	179	1.0	C131, U167, C168, C228, U231, G246, C247
R99C/C113A	174	242	1.0	C228, U231
C113 (wt)	100	134	0.05	n.d.[a]

Activity measurements: initial velocity measurements of protein holoenzyme pre-tRNA cleavage activity for wild-type P protein (C113, wt) and mutants F18C/C113A, H78C/C113A and R99C/C113A are shown. Maximum percent cleaved was 26%. Percent crosslinking efficiencies: efficiencies were calculated from duplicate experiments using 20 nM each RNase P protein and RNA. Protein–RNA crosslinks were resolved on 4% acrylamide/8 M urea/ TBE gels similar to that in Figure 3. RNA site crosslinked: crosslink sites for

F18C/C113A, H78C/C113A and R99C/C113A to RNase P RNA.

[a]The crosslink site for C113 was not determined due to low efficiency of crosslinking.

Open in new tab

References

1 Guerrier-Takada,C. and Altman,S. (1984) Catalytic activity of an RNA molecule prepared by transcription *in vitro*. *Science* , 223, 285–286.

Google Scholar

2 Guerrier-Takada,C., Gardiner,K., Marsh,T., Pace,N. and Altman,S. (1983) The RNA moiety of ribonuclease P is the catalytic subunit of the enzyme. *Cell* , 35, 849–857.

Google Scholar

3 Apirion,D. (1980) Genetic mapping and some characterization of the *rnpA*^{A49} mutation of *Escherichia coli* that affects the RNA-processing enzyme ribonuclease P. *Genetics* , 94, 291–299.

Google Scholar

4 Hansen,F.G., Hansen,E.B. and Atlung,T. (1985) Physical mapping and nucleotide sequence of the *rnpA* gene that encodes the protein component of ribonuclease P in *Escherichia coli*. *Gene* , 38, 85–93.

Google Scholar

5 Kurz,J.C., Niranjanakumari,S. and Fierke,C.A. (1998) Protein component of *Bacillus subtilis* RNase P specifically enhances the affinity for precursor-tRNA^{Asp}. *Biochemistry* , 37, 2393–2400.

Google Scholar

6 Tallsjö,A. and Kirsebom,L.A. (1993) Product release is a rate-limiting step during cleavage by the catalytic RNA subunit of *Escherichia coli* RNase P. *Nucleic Acids Res.* , 21, 51–57.

Google Scholar

7 Stams,T., Niranjanakumari,S., Fierke,C.A. and Christianson,D.W. (1998) Ribonuclease P protein structure: evolutionary origins in the translational apparatus. *Science* , 280, 752–755.

Google Scholar

8 Spitzfaden,C., Nicholson,N., Jones,J.J., Guth,S., Lehr,R., Prescott,C.D., Hegg,L.A. and

Eggleston,D.S. (2000) The structure of ribonuclease P protein from *Staphylococcus aureus* reveals a unique binding site for single-stranded RNA. *J. Mol. Biol.* , 295, 105–115.

Google Scholar

9 Chen,J.L., Nolan,J.M., Harris,M.E. and Pace,N.R. (1998) Comparative photocross-linking analysis of the tertiary structures of *Escherichia coli* and *Bacillus subtilis* RNase P RNAs. *EMBO J.* , 17, 1515–1525.

Google Scholar

10 Harris,M.E., Nolan,J.M., Malhotra,A., Brown,J.W., Harvey,S.C. and Pace,N.R. (1994) Use of photoaffinity crosslinking and molecular modeling to analyze the global architecture of ribonuclease P RNA. *EMBO J.* , 13, 3953–3963.

Google Scholar

11 Massire,C., Jaeger,L. and Westhof,E. (1998) Derivation of the three-dimensional architecture of bacterial ribonuclease P RNAs from comparative sequence analysis. *J. Mol. Biol.* , 279, 773–793.

Google Scholar

12 Loria,A., Niranjanakumari,S., Fierke,C.A. and Pan,T. (1998) Recognition of a pre-tRNA substrate by the *Bacillus subtilis* RNase P holoenzyme. *Biochemistry* , 37, 15466–15473.

Google Scholar

13 Talbot,S.J. and Altman,S. (1994) Gel retardation analysis of the interaction between C5 protein and M1 RNA in the formation of the ribonuclease P holoenzyme from *Escherichia coli*. *Biochemistry* , 33, 1399–1405.

Google Scholar

14 Vioque,A., Arnez,J. and Altman,S. (1988) Protein–RNA interactions in the RNase P holoenzyme from *Escherichia coli*. *J. Mol. Biol.* , 202, 835–848.

Google Scholar

15 Biswas,R., Ledman,D.W., Fox,R.O., Altman,S. and Gopalan,V. (2000) Mapping RNA–protein interactions in ribonuclease P from *Escherichia coli* using disulfide-linked EDTA-Fe. *J. Mol. Biol.* , 296, 19–31.

Google Scholar

16 Niranjanakumari,S., Stams,T., Crary,S.M., Christianson,D.W. and Fierke,C.A. (1998) Protein

component of the ribozyme ribonuclease P alters substrate recognition by directly contacting precursor tRNA. *Proc. Natl Acad. Sci. USA* , 95, 15212–15217.

Google Scholar

17 Waugh,D. (1989) *Mutational Analysis of Catalytic Function in Ribonuclease P RNA*. PhD thesis. Indiana University, Bloomington, IN.

Google Scholar

18 Nolan,J.M., Burke,D.H. and Pace,N.R. (1993) Circularly permuted tRNAs as specific photoaffinity probes of ribonuclease P RNA structure. *Science* , 261, 762–765.

Google Scholar

19 Rivera-Leon,R., Green,C.J. and Vold,B.S. (1995) High-level expression of soluble recombinant RNase P protein from *Escherichia coli*. *J. Bacteriol .*, 177, 2564–2566.

Google Scholar

20 Hanahan,D., Jessee,J. and Bloom,F.R. (1991) Plasmid transformation of *Escherichia coli* and other bacteria. *Methods Enzymol.* , 204, 63–113.

Google Scholar

21 Schagger,H. and von Jagow,G. (1987) Tricine-sodium dodecyl sulfate-polyacrylamide gel electrophoresis for the separation of proteins in the range from 1 to 100 kDa. *Anal. Biochem.* , 166, 368–379.

Google Scholar

22 Bradford,M.M. (1976) A rapid and sensitive method for the quantitation of microgram quantities of protein utilizing the principle of protein-dye binding. *Anal. Biochem.* , 72, 248–254.

Google Scholar

23 Pan,T. (1995) Higher order folding and domain analysis of the ribozyme from *Bacillus subtilis* ribonuclease P. *Biochemistry* , 34, 902–909.

Google Scholar

24 Smith,D. and Pace,N.R. (1993) Multiple magnesium ions in the ribonuclease P reaction mechanism. *Biochemistry* , 32, 5273–5281.

Google Scholar

25 Smith,D., Burgin,A.B., Haas,E.S. and Pace,N.R. (1992) Influence of metal ions on the

ribonuclease P reaction. Distinguishing substrate binding from catalysis. *J. Biol. Chem.* , 267, 2429–2436.

Google Scholar

26 Laemmli,U.K. (1970) Cleavage of structural proteins during the assembly of the head of bacteriophage T4. *Nature* , 227, 680–685.

Google Scholar

27 Talbot,S.J. and Altman,S. (1994) Kinetic and thermodynamic analysis of RNA–protein interactions in the RNase P holoenzyme from *Escherichia coli*. *Biochemistry* , 33, 1406–1411.

Google Scholar

28 Inoue,T. and Cech,T.R. (1985) Secondary structure of the circular form of the *Tetrahymena* rRNA intervening sequence: a technique for RNA structure analysis using chemical probes and reverse transcriptase. *Proc. Natl Acad. Sci. USA* , 82, 648–652.

Google Scholar

29 Haas,E.S., Morse,D.P., Brown,J.W., Schmidt,F.J. and Pace,N.R. (1991) Long-range structure in ribonuclease P RNA. *Science* , 254, 853–856.

Google Scholar

30 Harris,J.K., Haas,E.S., Williams,D., Frank,D.N. and Brown,J.W. (2001) New insight into RNase P RNA structure from comparative analysis of the archaeal RNA. *RNA* , 7, 220–232.

Google Scholar

31 Brown,J.W. (1999) The Ribonuclease P Database. *Nucleic Acids Res.* , 27, 314.

Google Scholar

32 Burgin,A.B. and Pace,N.R. (1990) Mapping the active site of ribonuclease P RNA using a substrate containing a photoaffinity agent. *EMBO J.* , 9, 4111–4118.

Google Scholar

33 Trang,P., Hsu,A.W. and Liu,F. (1999) Nuclease footprint analyses of the interactions between RNase P ribozyme and a model mRNA substrate. *Nucleic Acids Res.* , 27, 4590–4597.

Google Scholar

34 LaGrandeur,T.E., Huttenhofer,A., Noller,H.F. and Pace,N.R. (1994) Phylogenetic comparative

chemical footprint analysis of the interaction between ribonuclease P RNA and tRNA. *EMBO J.* , 13, 3945–3952.

Google Scholar

35 Harris,M.E., Kazantsev,A.V., Chen,J.L. and Pace,N.R. (1997) Analysis of the tertiary structure of the ribonuclease P ribozyme-substrate complex by site-specific photoaffinity crosslinking. *RNA* , 3, 561–576.

Google Scholar

36 Oh,B.-K. and Pace,N.R. (1994) Interaction of the 3′-end of tRNA with ribonuclease P RNA. *Nucleic Acids Res.* , 22, 4087–4094.

Google Scholar

37 Chen,J.L. (1997) *Structure of Ribonuclease P RNA*. PhD thesis. Indiana University, Bloomington, IN.

Google Scholar

38 Fang,X.W., Yang,X.J., Littrell,K., Niranjanakumari,S., Thiyagarajan,P., Fierke,C.A., Sosnick,T.R. and Pan,T. (2001) The *Bacillus subtilis* RNase P holoenzyme contains two RNase P RNA and two RNase P protein subunits. *RNA* , 7, 233–241.

Google Scholar

Issue Section: Article

Comments

0 Comments

Comments (0)

View Metrics

More on this topic

A screening platform to monitor RNA processing and protein-RNA interactions in ribonuclease P uncovers a small molecule inhibitor

In vivo and *in vitro* investigation of bacterial type B RNase P interaction with tRNA 3′-CCA

A universal RNA structural motif docking the elbow of tRNA in the ribosome, RNAse P and T-box leaders

Enzymatic synthesis of the TΨ-loop analog of yeast tRNA1^{Val}

Related articles in

Web of Science

Google Scholar

Related articles in PubMed

Arterial wall structural changes in noncirrhotic chronic hepatitis C patients.

Clinicopathological characteristics of Epstein-Barr virus-positive gastric cancer in Latvia.

Hexokinase II up-regulation contributes to asiaticoside-induced protection of H9c2 cardioblasts during oxygen-glucose deprivation/reoxygenation.

Self-assembly of poly(allylamine)/siRNA nanoparticles, their intracellular fate and siRNA delivery.

Citing articles via

Web of Science (20)

Google Scholar

Crossref

Latest | **Most Read** | **Most Cited**

Structural insights into synthetic ligands targeting A–A pairs in disease-related CAG RNA repeats

Poly(ADP-ribose)-dependent chromatin unfolding facilitates the association of DNA-binding proteins with DNA at sites of damage

OGRDB: a reference database of inferred immune receptor genes

AID–RNA polymerase II transcription-dependent deamination of IgV DNA

Cell-free expression of RNA encoded genes using MS2 replicase

About Nucleic Acids Research
Editorial Board
Policies
Author Guidelines
Facebook
Twitter
LinkedIn
Advertising and Corporate Services
Journals Career Network

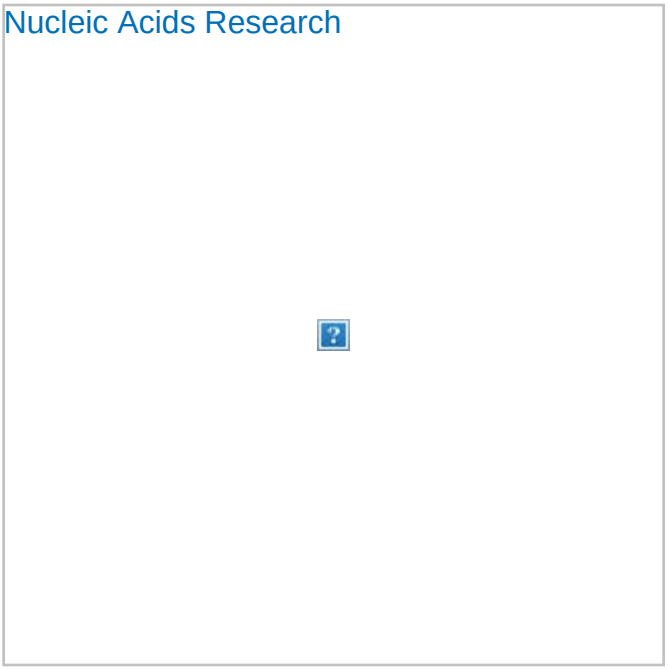

Online ISSN 1362-4962
Print ISSN 0305-1048

and education by publishing worldwide